Electronic Supplementary Material (ESI) for Soft Matter.

Online Supplement for *Drop ejection from vibrating damped, dampened wings*

1 Supplementary movie captions

Movie S1: Sliding ejection mode. A mobile drop slides from its initial position to the end of the cantilever, and leaves no portion of itself on the substrate.
Movie S2: Normal-to-substrate ejection. A drop ejects without sliding from its original position, with nearly symmetrical contact line motion, and leaves no portion of itself on the substrate.
Movie S3: Pinch-off ejections. A portion of the drop ejects in cohesive failure while a portion of the drop remains attached to the substrate. The drop deforms to form a neck which closes in one of three ways: neck closure at the portion attached to the substrate, neck closure at the ejecting mass, and simultaneous closure at both liquid bodies.
Movie S4: Comparison of actual cantilever deflection to theoretical deflection simulated and animated with MATLAB. Axes in the simulated motion have units of meters (m).

2 Determining inertial forces from modal shape

The traditional approach to beam structural dynamics theory involves the Euler-Bernoulli kinematic assumption with small deflections and provides a straightforward path from a statement of equilibrium to the equation of motion. However, the large deflections observed motivate the use of Euler's elastica to model the beam deformation. In addition, the presence of fluid drops atop the beams imposes added forcing/inertial terms. Using representative static solutions of the elastica as a nonlinear basis for the large deflections, a reduced-order energy-based model admits a path to predict the beam structural dynamics through an assumed-modes model. Finally, we can use the elastica kinematics to transform the beam's structural dynamics to the drop's motion and thus associated inertial forces.

2.1 Elastica development

A beam's bending moment M is proportional to the change in the curvature produced by the action of the load **Fig.S3**. This law may be written mathematically as follows:

$$\frac{1}{r} = -\frac{d\theta}{dz} = -\frac{M}{EI} \tag{1}$$

where r is the radius of curvature, θ is the slope at any point x_o, where x_o is measured along the arc length of the member as shown in **Fig.S3**, E is the modulus of elasticity, and I is the cross-sectional moment of inertia.

Looking ahead, we represent the beam's transverse deflection as a representative static shape $w_{\text{am}}(x)$. In Cartesian coordinates, Eq.(1) may then be written as

$$\frac{1}{r} = \frac{w''_{\text{am}}}{[1+(w'_{\text{am}})^2]^{\frac{3}{2}}} = -\frac{M}{EI} \tag{2}$$

where

$$w'_{\text{am}} = \frac{dw_{\text{am}}}{dx} \qquad \text{and} \qquad w''_{\text{am}} = \frac{d^2 w_{\text{am}}}{dx^2}. \tag{3}$$

The expression for the bending moment M at any $0 \leq x \leq x_{\text{f}}$, where x_{f} tip-to-base distance for a curved beam of length L, may be obtained by using the free-body diagram in **Fig.S3**. Applying statics,

$$M = -P(x_{\text{f}} - x). \tag{4}$$

By substituting Eq.(4) into Eq.(2) and assuming that the flexural rigidity EI is uniform along the beam length, we obtain

$$\frac{w''_{\text{am}}}{[1 + (w'_{\text{am}})^2]^{\frac{3}{2}}} = \frac{P(x_{\text{f}} - x)}{EI} \equiv \lambda(x). \tag{5}$$

Integrating Eq.(5), we obtain

$$\frac{w'_{\text{am}}}{[1 + (w'_{\text{am}})^2]^{\frac{1}{2}}} = \varphi(x) + C, \tag{6}$$

where

$$\varphi(x) = \int \lambda(x) dx = \frac{P}{EI}(x_{\text{f}} x - \frac{1}{2} x^2) \tag{7}$$

and C is the constant of integration that can be determined by applying a boundary condition. In this case the beam has zero slope at the root, or $w'_{\text{am}}(0) = 0$. By using this boundary condition in Eq.(6), we find

$$\frac{w'_{\text{am}}}{[1 + (w'_{\text{am}})^2]^{\frac{1}{2}}} = \frac{P}{EI}(x_{\text{f}} x - \frac{1}{2} x^2) \equiv G(x). \tag{8}$$

Solving Eq.(8) for w'_{am}, we obtain

$$w_{\text{am}}{}'(x) = \frac{G(x)}{[1 - G(x)^2]^{\frac{1}{2}}}. \tag{9}$$

It should be noted, however, that $G(x)$ in Eq.(8) is a function of the unknown horizontal displacement $\Delta = L - x_{\text{f}}$ of the free end of the beam. The value of Δ may be determined from the equation

$$L = \int_0^{x_{\text{f}}} [1 + (w'_{\text{am}})^2]^{\frac{1}{2}} dx \tag{10}$$

by using a shooting method. That is, we assume a value of Δ (and thus x_{f}, the upper limit of integration) and carry out the integration in Eq.(10). If our guess of Δ is correct, the integral will indeed yield the beam length L. If the integral is too large, our calculated beam length is too long and we need to use a smaller Δ; if the integral is too small, a larger Δ. The procedure may be repeated for various values of Δ until the correct length L is obtained; numerical methods exist to carry out this procedure rapidly and to ensure convergence to the actual beam length.

Building on this method, we then use the results of Eq.(10) to find the corresponding assumed horizontal deformation of the beam, which we describe as the deflection in the negative x-direction u_{am}. Moreover, we can apply the method for any given point on the beam, not merely for the full length. In so doing, we establish a numerical assumed shape for the horizontal deformation. With u_{am} found, w_{am} can be found using Eq.(5). Eq.(5) is a nonlinear second order differential equation and exact solution of this equation is not presently available[1]. Instead we use a Taylor series expansion taking only the first two terms of the series and then converge it with the original equation. Convergence of these two equations shows that the difference is on the order of $O(-15)$.

2.2 Reduced-order energy-based model development

Using an assumed-modes construction, we represent the beam displacement in terms of the representative deflection shape $w_{\mathrm{am}}(x)$ (i.e., the assumed mode derived above) and a rigid-body displacement mode $w_0(x)$. While this approach admits the inclusion of additional assumed modes, we found a single-mode approximation adequately predicts the beam dynamics. The total beam transverse displacement is then

$$w(x,t) = a_0(t)w_0(x) + a(t)w_{\mathrm{am}}(x), \tag{11}$$

where $a(t)$ represents the amplitude of the assumed mode motion and $a_0(t)$ corresponds to the vertical motion of the shaker (i.e., the beam root). The total beam axial displacement

$$u(x,t) = a_0(t)u_0(x) + a(t)u_{\mathrm{am}}(x). \tag{12}$$

The experiments involve base excitation of the beams, so we use $w_0(x) = 1$. Base motion is strictly transverse to the beam, so the horizontal component $u_0(x) = 0$.

Formulating the equations of motion involves application of the extended Hamilton's Principle, which involves computations of the kinetic energy, strain energy, and virtual work associated with a virtual displacement within a particular assumed mode[2]. The kinetic energy of the beam is

$$T = \frac{1}{2}\int_0^L \rho A\left(\dot{u}(x,t)^2 + \dot{w}(x,t)^2\right)dx. \tag{13}$$

Substituting the assumed-modes representations of Eqs. (11) and (12) and recognizing that $a(t)$ and $a_0(t)$ can be pulled outside the spatial integrals:

$$T = \frac{1}{2}\left[\dot{a}^2\left(\int_0^L \rho A u_{\mathrm{am}}^2 dx + \int_0^L \rho A w_{\mathrm{am}}^2 dx\right) + \dot{a}_0^2\int_0^L \rho A w_0^2 dx + 2\dot{a}_0\dot{a}\int_0^L \rho A w_0 w_{\mathrm{am}} dx\right]. \tag{14}$$

Note this has a quadratic form

$$T = \frac{1}{2}\begin{Bmatrix}\dot{a}_0\\ \dot{a}\end{Bmatrix}^t \begin{bmatrix}M_{00} & M_0\\ M_0^t & M\end{bmatrix}\begin{Bmatrix}\dot{a}_0\\ \dot{a}\end{Bmatrix}, \tag{15}$$

where

$$M = \int_0^L \rho A u_{\mathrm{am}}^2 dx + \int_0^L \rho A w_{\mathrm{am}}^2 dx \qquad \text{and} \qquad M_0 = \int_0^L \rho A w_0 . w_{\mathrm{am}} dx. \tag{16}$$

The strain energy of the beam, including non-linear strain-displacement relations to account for the large displacements and rotations, is

$$U = \frac{1}{2}\int_0^L \left[(EIw''(x))^2 + \frac{1}{2}(EIw'(x,t))^2(w''(x))^2 + \frac{1}{320}Ebh^5(w''(x,t))^4\right]dx, \tag{17}$$

where b is beam with and h is beam thickness. Since the base motion is a rigid-body motion, the spatial derivatives $w_0' = w_0'' = \cdots = 0$ and we only have derivatives of the assumed modes. As with the kinetic energy, the time component $a(t)$ can be pulled outside the integral and for a single-term approximation:

$$U = \frac{1}{2}a^2 \int_0^L EI(w''_{\text{am}})^2 dx + \frac{1}{4}a^4 \int_0^L EI(w'_{\text{am}})^2(w''_{\text{am}})^2 dx + \frac{1}{640}a^4 \int_0^L Ebh^5(w''_{\text{am}})^4 dx. \tag{18}$$

In computing these derivatives, we use a finite-difference method; the derivatives of u'_{am} and w''_{am} are shown in **Fig.S4** to confirm smoothness. One term of this expression has a quadratic form, which leads to

$$U = \frac{1}{2}\begin{Bmatrix} a_0 \\ a \end{Bmatrix}^t \begin{bmatrix} 0 & 0 \\ 0 & k_{\text{L}} \end{bmatrix} \begin{Bmatrix} a_0 \\ a \end{Bmatrix} + \frac{1}{4}\begin{Bmatrix} a_0 \\ a \end{Bmatrix}^t \begin{bmatrix} 0 & 0 \\ 0 & k_{\text{NL}} \end{bmatrix} \begin{Bmatrix} a_0^3 \\ a^3 \end{Bmatrix}. \tag{19}$$

Eq.(18) can be divided into two parts: the usual linear stiffness from Euler-Bernoulli beam theory (quadratic energy term) and the nonlinear stiffness terms:

$$k_{\text{L}} = \int_0^L EI{w''_{\text{am}}}^2 dx, \tag{20}$$

and from Von Karman strain the non-linear term is:

$$k_{\text{NL}} = \int_0^L \left[EI{w'_{\text{am}}}^2{w''_{\text{am}}}^2 + \frac{1}{160}Ebh^5{w''_{\text{am}}}^4 \right] dx. \tag{21}$$

Finally, the beam is driven via harmonic base motion, $f_{\text{base}}(t)$. Since it is applied only at the root of the beam, the virtual work associated with this forcing is

$$\delta W = f_{\text{base}}(t)\delta w(0,t) = f_{\text{base}}(t)\delta a_0(t)w_0(0) + f_{\text{base}}(t)\delta a(t)w(0) = \delta a_0(t)f_{\text{base}}(t). \tag{22}$$

Application of extended Hamilton's Principle then leads to a set of equations of motion:

$$\begin{bmatrix} M_{00} & M_0 \\ M_0^t & M \end{bmatrix} \begin{Bmatrix} \ddot{a}_0 \\ \ddot{a} \end{Bmatrix} + \begin{bmatrix} 0 & 0 \\ 0 & k_{\text{L}} \end{bmatrix} \begin{Bmatrix} a_0 \\ a \end{Bmatrix} + \begin{Bmatrix} 0 \\ k_{\text{NL}}a^3 \end{Bmatrix} = \begin{Bmatrix} f_{\text{base}} \\ 0 \end{Bmatrix} \tag{23}$$

The experiments involve base motion that consists of a fixed-frequency oscillation with linearly increasing amplitude; that is,

$$a_0(t) = (A_{\text{i}} + A_{\text{rate}}t)\sin\Omega t, \tag{24}$$

where A_{i} is the initial base amplitude and A_{rate} is the rate at which the base amplitude increases. With the addition of a viscous damping term for the beam, the second equation of Eq.(23) becomes

$$M\ddot{a} + c\dot{a} + k_{\text{L}}a + k_{\text{NL}}a^3 = -M_0\ddot{a}_0(t) \tag{25}$$

Solving Eq.(25) yields $a(t)$ and substituting back in Eqs. (11), (12) and (24) provides the beam axial and transverse displacement:

$$u(x,t) = a(t)u_{\text{am}}(x) \tag{26}$$

and

$$w(x,t) = a(t)w_{\text{am}}(x) + (A_{\text{i}} + A_{\text{rate}}t)\sin(\Omega t). \tag{27}$$

2.3 Kinematics and drop motion

With the beam motion determined, we can compute the drop motion and its associated inertial forces. Here, x_0 is the position of the drop when the beam is stationary, which is labeled in **Fig.4** of the main text. Using Eq.(26) the horizontal displacement of the point where the drop contacts the beam becomes:

$$x_{\mathrm{d}}(t) = x_0 - a(t)u_{\mathrm{am}}(x_0) \tag{28}$$

The vertical displacement of the point where the drop contacts the beam is simply the displacement at that point, $y_{\mathrm{d}}(t) = w(x_0, t)$. From Eq.(27), Eq.(28), and **Fig.4** of the main text, the position vector $\mathbf{r}(t)$ of the point mass is:

$$\begin{aligned}
\mathbf{r}(t) &= \left[x_{\mathrm{d}} - \delta \sin w'(x_0, t)\right] \hat{\imath} + \left[y_{\mathrm{d}} + \delta \cos w'(x_0, t)\right] \hat{\jmath} && (29)\\
&= \left[x_0 - a u_{\mathrm{am}} - \delta \sin w'(x_0, t)\right] \hat{\imath} + \left[a w_{\mathrm{am}} + (A_{\mathrm{i}} + A_{\mathrm{rate}} t)\sin(\Omega t) + \delta \cos w'(x_0, t)\right] \hat{\jmath}. && (30)
\end{aligned}$$

Finally, the inertial force acting on a rigid drops center of mass (COM) is

$$F_i = m_{\mathrm{d}} \ddot{\mathbf{r}}. \tag{31}$$

3 Droplet volume

The droplet radius, $R(h)$ shown in **Fig.S5**, which is dependent on the height, h, can be described at an arbitrary height by [3]:

$$R(h) = \sqrt{R^2 - (h - R\cos\theta_{\mathrm{e}})^2}. \tag{32}$$

The volume of a droplet with equilibrium contact angle θ_{e} can be calculated as follows:

$$V = \frac{4}{3}\pi R^3 - \int_0^{2R-H} \pi R(h)^2 dh. \tag{33}$$

Representing the upper limit of the integration, $h' = 2R - H$,

$$V = \pi \left[\frac{4}{3}R^3 - R^2 h' + \frac{(h')^2}{3} - (h')^2 \cos\theta_{\mathrm{e}} + R^2 h' \cos^2\theta_{\mathrm{e}}\right]. \tag{34}$$

4 Supplementary figures

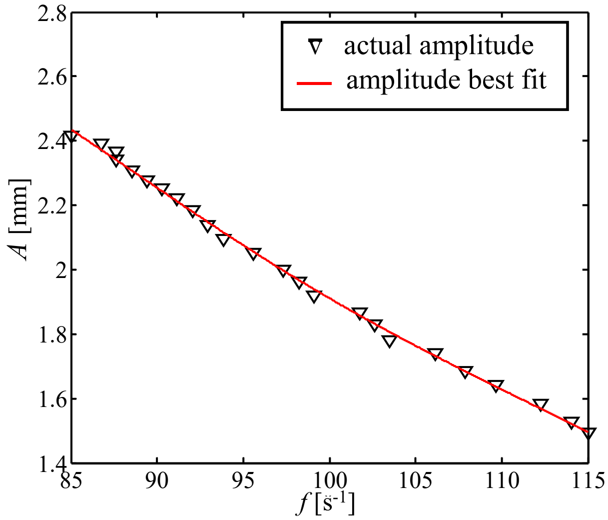

Figure S1: Shaker base amplitude across the range of experimental vibration frequency.

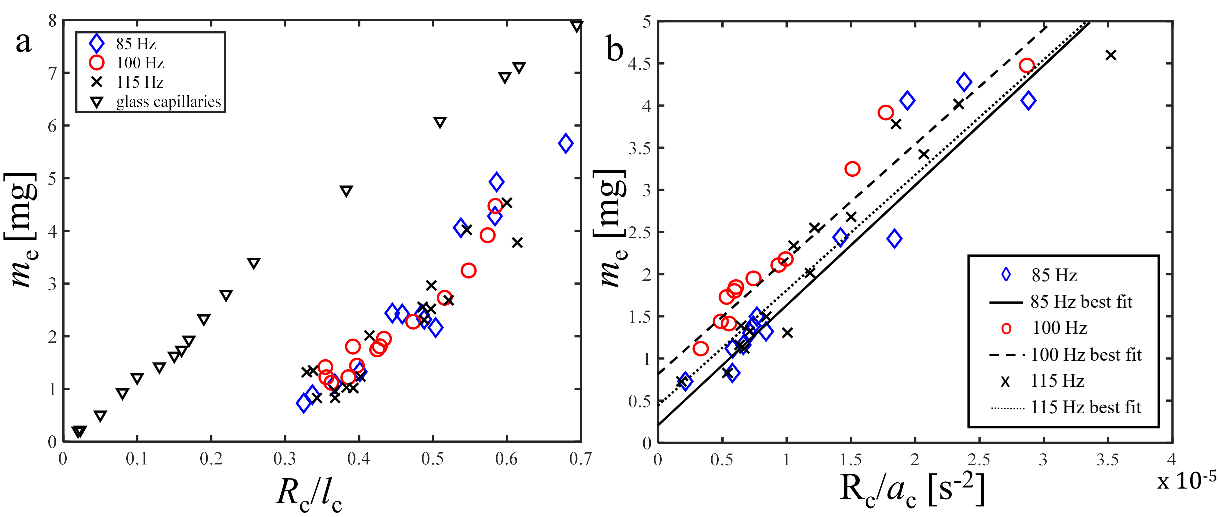

Figure S2: Drop release via pinch-off. (a) The dependence of released mass and the size of the drop. The mass of drops dripping from glass capillaries is shown for comparison [4]. (b) The relation between drop mass and cantilever acceleration of drop release. Best fits in (b) are given by **Eq.7** (main text) using $F(R_c, x_o, \theta_e)$ 0.34, 0.29, and 0.30 for 85 Hz, 100 Hz, and 115 Hz respectively.

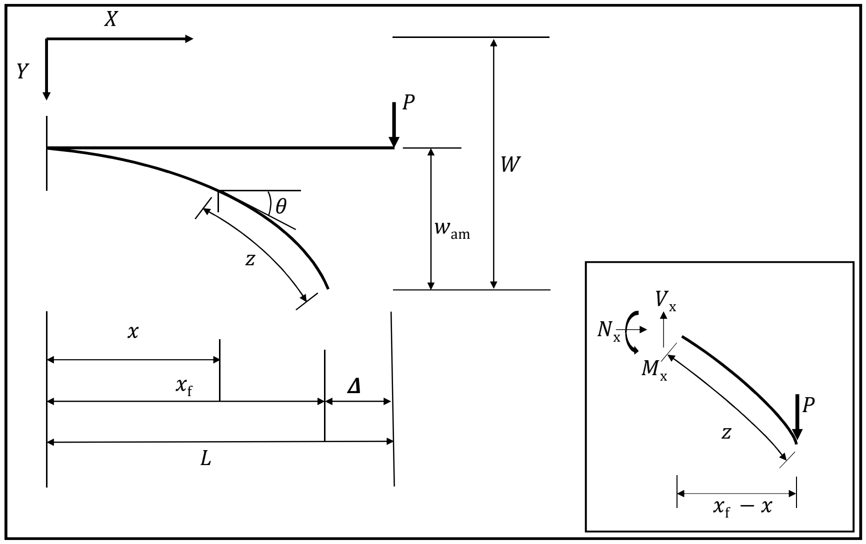

Figure S3: Large deformation of a cantilever beam of uniform cross section. Inset: Free-body diagram of a beam element of arbitrary length.

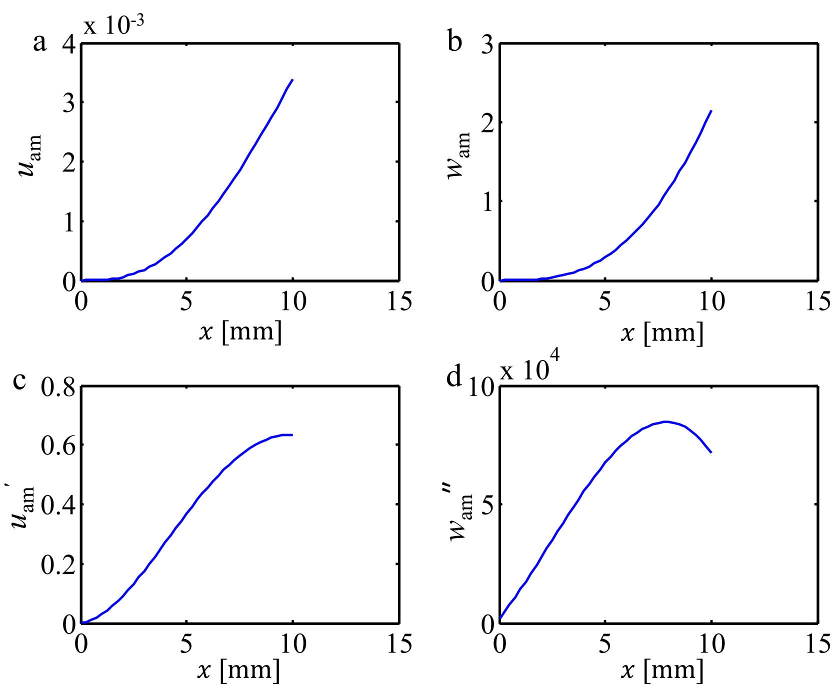

Figure S4: Assumed beam deflection shapes in the (a) axial and (b) transverse directions for all points along the beam length, with (c) and (d) spatial derivatives used in strain energy formulation.

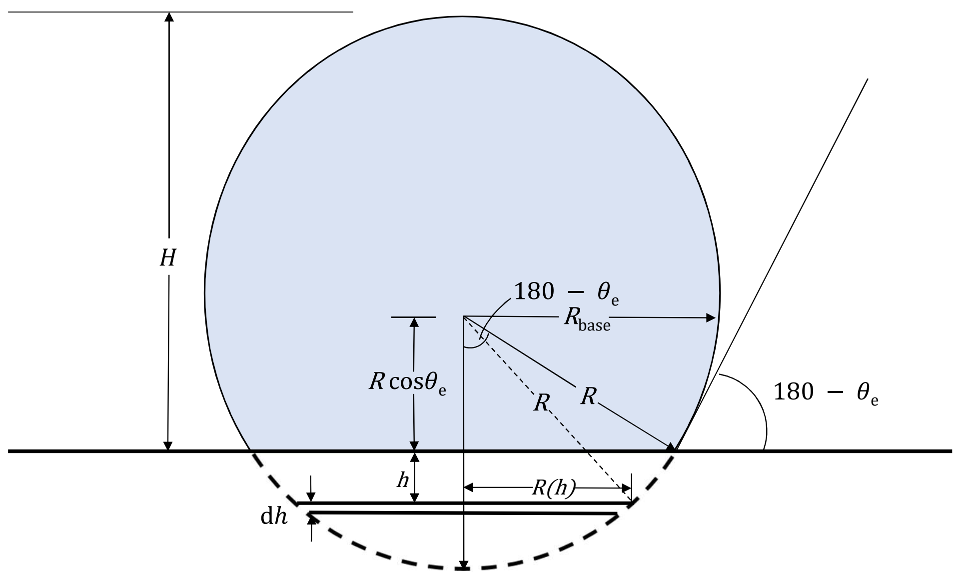

Figure S5: Geometric description for calculating the volume of a drop resting on a flat surface.

References

[1] Fertis, D. G., 2006 *Nonlinear structural engineering*. Springer.

[2] Meirovitch, L., 1997 *Principles and Techniques of Vibrations*. Upper Saddle River, NJ: Prentice Hall.

[3] Kim, Y. H., Kim, K. & Jeong, J. H., 2016 Determination of the adhesion energy of liquid droplets on a hydrophobic flat surface considering the contact area. *International Journal of Heat and Mass Transfer* **102**, 826–832.

[4] Harkins, W. & Brown, F., 1919 The determination of surface tension (free surface energy), and the weight of falling drops: the surface tension of water and benzene by the capillary height method. *Journal of the American Chemical Society* **41**, 499–524. ISSN 0002-7863.